Ryszard Korycki,
***Henryk Kapusta**

Optimization of the Thickness of Layers within a Calender Shaft

DOI: 10.5604/12303666.1152743

Department of Technical Mechanics and Computer Science,
Lodz University of Technology,
ul. Żeromskiego, 116; 90-924 Łódź, Poland
E-mail: ryszard.korycki@p.lodz.pl

Research and Development Centre of Textile Machinery "Polmatex-Cenaro",
ul. Wolczanska, 55/59; Łódź, Poland

Abstract
Calenders are widely used in the textile industry to finish flat textile products. The main goal of the paper was to analyze the thermal phenomena within a calender shaft heated by oil and optimize the material thickness and distribution of heat sources within the external mantle. The optimization problem is solved by means of both sensitivity and the material derivative concept. Characteristics of the state variable (i.e. the temperature of the mantle surface) are determined as time-dependent. Numerical examples of material layer optimization are also included.

Key words: *soybean fibre, regenerated fibre, dyeing properties, biodegradable fibre, sustainable products, functional properties, flame resistance.*

Nomenclature

- $\mathbf{A}$ *matrix of thermal conduction coefficients, $Wm^{-1}K^{-1}$*
- $\mathbf{b}$ *vector of design parameters, m*
- C *constraint functional, in this case the global cost of the structure, -*
- C_0 *imposed constant value of the constraint functional (structural cost), -*
- f *heat source capacity, Wm^{-1}*
- c *volumetric heat capacity, $Jkg^{-1}K^{-1}$*
- F *objective functional, -*
- F' *Lagrange functional (the auxiliary function), -*
- $g_p = Dg/Db_p$ *global (material) derivative of g with respect to design parameter b_p, -*
- $g^p = \partial g/\partial b_p$ *partial (local) derivative of g with respect to design parameter b_p, -*
- H *mean curvature of external boundary Γ, m^{-1}*
- H_s *spiral lead, m*
- h *surface film conductance, $Wm^{-2}K^{-1}$*
- $\mathbf{n}$ *unit vector normal to the external boundary Γ, directed outwards to the domain Ω bounded by this boundary, -*
- n_s *turn number of spring, -*
- P *number of design parameters during sensitivity analysis, -*
- $\mathbf{q}$ *vector of the heat flux density, Wm^{-1}*
- $\mathbf{q}^*$ *vector of the initial heat flux density, Wm^{-1}*
- $q_n = \mathbf{n}\cdot\mathbf{q}$ *heat flux density normal to the external boundary, Wm^{-1}*
- R *radius of screw line/spring, m*
- T *temperature, °C*
- T^0 *prescribed value of temperature, °C*
- T_{0L} *assumed level of the temperature, °C*
- T *temperature of the surroundings, °C*
- t *real time in the primary and additional structures, s*
- t_s *spring turn parameter, -*
- u *unit cost of the structure,*
- $\mathbf{v}^p(\mathbf{x},\mathbf{b},t)$ *transformation velocity field associated with design parameter b_p,*
- $v_n^p = \mathbf{n}\cdot\mathbf{v}^p$ *transformation velocity normal to the external boundary Γ,*
- $\mathbf{v}_\Gamma^p$ *transformation velocity vector in the plane tangent to the external boundary Γ,*
- x *vector of points' coordinates, m*
- Γ *external boundary of the structure, -*
- β *coefficient linking temperature and time, 1 °C s^{-1}*
- γ *boundary integrand of the objective functional, -*
- $\gamma_{,(\cdot)} = \partial\gamma/\partial_{(\cdot)}$ *partial (local) derivative of boundary integrand of the objective functional in respect of $(\cdot)$, -*
- $\gamma_{,n}$ *partial (local) derivative of boundary integrand of the objective functional in respect of the direction normal to the external boundary Γ (defined as a space problem), -*
- ε *effective porosity of the textile material, -*
- ξ *slack variable of the Lagrange functional for the inequality problems, -*
- Σ *discontinuity line between adjacent parts of the piecewise smooth boundary Γ, -*
- σ *Stefan-Boltzmann constant, density of fibre, kg m^{-3}*
- τ *transformed time in the adjoint structure, s*
- υ *unit vector tangent to both portions of the smooth external boundary Γ, -*
- χ *Lagrange multiplier, -*
- Ψ *domain integrand of the objective functional, -*
- Ω *domain of the structure, m^2*
- ∇ *gradient operator, -*

Introduction

Calenders are widely used in the textile industry to finish/smooth flat textile products i.e. woven fabrics, knitted fabrics and non-wovens. Calenders are included into the group of winding machines. Their primary task is to give forming products some relevant parameters, e.g. strength, thickness, width, cohesiveness, smoothness etc. The smoothing of materials as well as consolidation of multilayer textile composites made of non-wovens is based on strong pressure by the shaft at a high temperature. The temperature of the shaft surface depends

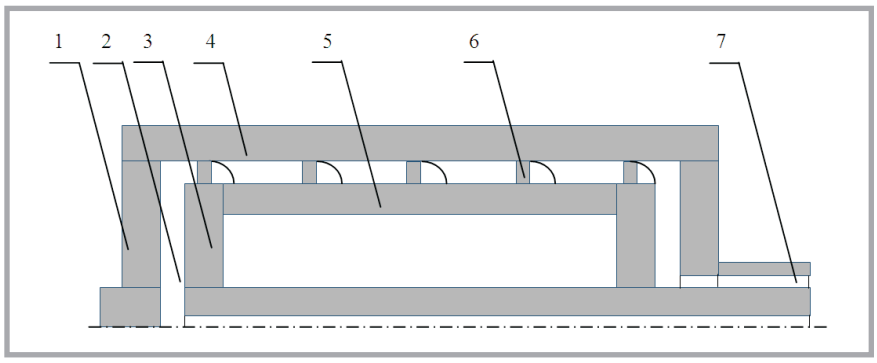

Figure 1. *Scheme of oil-heated calender shaft (a half of cross-section); 1 – external disk protection, 2 – oil inlet channel, 3 – internal disk protection, 4 – external mantle, 5 – internal mantle, 6 – spiral rib, 7 – oil outlet channel.*

on the forming material, with a typical value being between 200 °C and 300 °C.

The calender operates continuously, but relatively rarely in a transient state (no longer than 2 hours) particularly durin the starting and braking of the device. Heating of the shaft to a specific temperature requires a relatively long time. The temperature difference along the operating surface required during steady heat transport should be negligible, i.e. maximally a few degrees Celsius. Operating conditions should be constant irrespective of external disturbances during the whole smoothing process. This is particularly important in the welding process of multi-layer nonwoven composites and composites containing films or powders of special properties. Thus the basic problem is always to secure the constant temperature of shaft surface. Other parameters such as the pressure force of the shaft, velocities etc. are easy to control.
A calender shaft is composed of three heating zones. The central zone is a basic heating part of equalized temperature. The side zones are the reheating parts. Simulation of thermal processes within the shaft as well as that of regulation and control of heating zones play an important role in the design and operation of these machines.

Calenders are often used as thermal stabilizers during different textile engineering processes. The structural changes and mechanical properties of spun-bonded polylactide (PLA) nonwovens were examined by Sztajnowski, Krucinska et al. [1]. These nonwovens were stabilized on a calender at various temperatures ranging from 60 to 110 °C. Puchalski, Krucinska et al. [2] determined the influence of the calender temperature on the crystallization behaviour of polylactide (PLA) non-woven fabrics during their manufacturing by the spun-bonding technique. The structural rebuild of PLA presented explains changes observed in the physical–mechanical properties of non-woven fabrics obtained at different calendering temperatures. Control of the amount of deformation produced by the pressing and pressed rollers is crucial in order to optimize the quality of output of the calender. Kuo and Fang [3] modelled the pressed roller of a calender as a distributed system with an infinite number of degrees of freedom. The major objectives of this study was to control the pressed roller of a calender, without the need for both the pressed and pressing rollers, to enable the amount of convexity to be adjusted online, which in turn permits the leveling of the contact surface between the calender pressing roller and the calender pressed roller during processing. According to Kuo and Tu [4], to estimate the optimization parameters with multiple quality characteristics, gray relational analysis was incorporated to set quality characteristics as reference sequences and decide on the optimal parameter combinations. The quality characteristics included the reflectance, water vapour permeability and colour difference of calendered fabrics. The effect of calendering and sandwiching hollow polyester fibers between two layers of fine polyester fibers on the abrasion resistance and fabric stiffness was studied by Midha [5]. Although calendering improves fabric abrasion resistance properties, fabric stiffness increases. The main problem is the nonuniform temperature distribution on the working surface along the calendar axis. Optimal design of the heat distribution, leading to uniform temperature ofa given value, is analysed by Turant [6] using an evolutionary algorithm, whereas the calender is analyzed at the analysis stage by the finite element method.

There is a number of heating systems of calender shafts used in industry. Most used is water vapor at high temperature, which requires a typical heat distribution network or steam generator. Thus devices supplying steam and a condensate drain are necessary in this case. The shaft can be also heated by means of electric heaters, which requires a constant supply of electricity. Let us heat the calender shaft by means of oil (***Figure 1***). This solution is economical, because heat losses are minimal. The decrease in the oil temperature is negligible, only a few to several tens of degrees Celsius. The oil heating system requires neither a water vapor supply nor current refilling. The device operates in a dual-action system: initial phase - working with full power, and normal operation - operating only a support temperature system. Calender shafts have two mantles: external and internal. Between these mantles is a spiral flow channel which forces the resultant motion of the heating factor in the longitudinal and circumferential direction. The rotary motion of the shaft generates a centrifugal force that provides a good adhesion of oil to the outer mantle. In addition, the movement of oil is forced by the differential pressure between the input and output. The flow is turbulent, which still supports the heat transfer.

The main goal of the paper was to analyze the thermal phenomena within a calender shaft heated by oil as well as optimize the material layers within the external mantle. The optimization problem is solved by means of both the sensitivity and material derivative concept. The direct and adjoint approaches to sensitivity analysis are also considered, cf. Dems, Korycki [9], Dems, Korycki, Rousselet [7], Korycki [8, 10, 11]. Some problems concerning radiation are introduced, for example, by Korycki [8, 10]. Li [12] discussed the parameters describing combined conduction and radiation. The solution is sensitivity oriented and contains the sensitivities of the state fields as well as the sensitivity expressions within the structure. The sensitivity oriented optimization of material thickness and selected dimensions in the calender mantle as well as studies concerning the application of various materials including hybrid materials are not yet found in the literature analysed. Characteristics of the state variable (i.e. temperature of

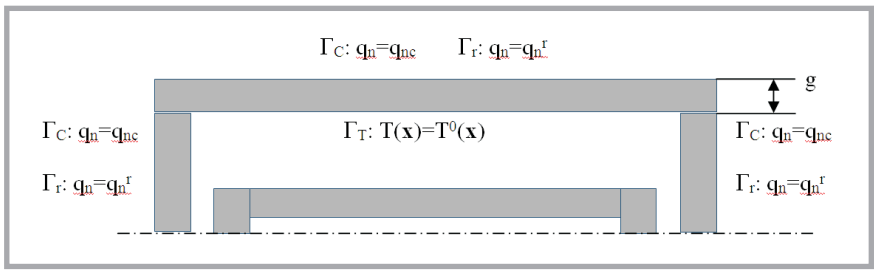

Figure 2. *Boundary conditions of one-layer calender mantle.*

the mantle surface) are determined as time-dependent. Available literature does not contain a description of temperature distribution as a state variable, numerical simulation of heat transfer for different materials, sensitivity analysis, nor combined optimization of material thickness and heat source distribution with respect to the calender shaft.

Physical and mathematical description

The state variable is the temperature T. The transient heat transport described in general by Korycki [8, 10] can be partially simplified. The problem is accompanied by a set of boundary and initial conditions. In order to optimize the material thickness, let us first expand the helix/screw line i.e. the central line of the channel with heating oil. Let us also assume that the screw line has a radius $R > 0$, spiral lead $H > 0$ and parameter $0 \le t_S \le 2\Pi$. The parameter equation and length can be described in the Cartesian coordinate system as shown in ***Equation 1***:

$$\begin{cases} x = R\cos t; \\ y = R\sin t; \\ z = n_S H_S t_S; \end{cases} \qquad L = 2\Pi\sqrt{R^2 + H_S^2} \quad (1)$$

Let us first optimize the classical structure of a calender made of a single external metallic mantle as well as multilayer materials. The structure contacts the heating oil, and the boundary is also the portion $_T$ subjected to the first-kind condition, cf. ***Figure 2***. The external and side boundary portion $_C$ and $_r$ is subjected to the global third kind as well as radiational conditions, i.e. convectional and radiational heat fluxes. The fourth-kind boundary conditions are defined for the common surfaces of internal boundary $_N$, for example between the different material layers etc. The heat flux density normal to this boundary portion $_N$ has the same value. The initial condition determines the temperature distribution within the optimized structure. The primary problem is defined according to [8, 10] for material layer I (see ***Equation 2***).

The problem can be considerably simplified for the steady heat transfer. The time derivative of the temperature with respect to time is negligible.

Sensitivity oriented optimization

Let us consider an arbitrary behavioral functional associated with the transient heat transfer problem, described within the structure as shown in ***Equation 3***.

$$F = \int_0^{t_k}\left[\int_\Gamma \gamma(T, q_n, T_\infty)\,d\Gamma\right]_i dt \qquad (3)$$

where Ψ and γ are continuous and differentiable functions of their arguments. According to the material derivative concept, the first-order sensitivity of the objective functional is assumed as the material derivative with respect to the design parameter. The sensitivity can be analyzed using the direct and adjoint approaches, respectively.

Let us first determine the direct approach. The unknown sensitivities of state fields are obtained by means of the additional structure associated with each design parameter. This approach is useful for calculating the sensitivities of the entire response field with respect to a few design variables. The number of problems to solve is equal to that of the design parameters and additionally the primary problem. The additional structure has the same shape as well as thermal and radiation properties as the primary one. It is characterized by the correlations determined by the differentiation of primary equations with respect to design parameters. The state equation and set of conditions are characterized according to [8, 10] for material layer 'i' (***Equation 4***).

The first-order sensitivity expression can be expressed as in ***Equation 5***, cf. [8, 10].

The symbol $\left]\gamma \mathbf{v}^p \cdot \upsilon\right[$ denotes a jump of the product within brackets calculated as a difference between two sides of the external boundary Γ along the discontinuity line Σ.

The alternative adjoint approach requires the solution of the adjoint and primary heat transfer problems. The adjoint and primary structures have the same shape as well as thermal and radiation properties. The adjoint method is the most convenient for estimating first-order sensitivities with respect to a few objective functionals. The heat conduction equation as well as the boundary and initial conditions can be defined with respect to Korycki [8, 10], (see ***Equation 6***).

$$\begin{cases} -\operatorname{div}\mathbf{q}^{(i)} + f^{(i)} = c^{(i)}\dfrac{dT^{(i)}}{dt} & \mathbf{x}\in\Omega; \\ \mathbf{q}^{(i)} = \mathbf{A}^{(i)}\cdot\nabla T^{(i)} + \mathbf{q}^{*(i)} \end{cases}$$
$$\begin{aligned} &T(\mathbf{x},t) = T^0(\mathbf{x},t) \quad \mathbf{x}\in\Gamma_T; \quad q_n^r(\mathbf{x},t) = \sigma\, T(\mathbf{x},t)^4 \quad \mathbf{x}\in\Gamma_r \\ &q_{nc}(\mathbf{x},t) = h\left[T(\mathbf{x},t) - T_\infty(\mathbf{x},t)\right] \quad \mathbf{x}\in\Gamma_C; \\ &q_n^{(i)}(\mathbf{x},t) = q_n^{(i+1)}(\mathbf{x},t) \quad \mathbf{x}\in\Gamma_N; \\ &T(\mathbf{x},0) = T_0 \;; \quad \mathbf{x}\in(\Omega\cup\Gamma). \end{aligned} \qquad (2)$$

$$\begin{cases} -\operatorname{div}\mathbf{q}^{p(i)} + f^{p(i)} = c^{(i)}\dfrac{dT^{p(i)}}{dt} & \mathbf{x}\in\Omega; \\ \mathbf{q}^{p(i)} = \mathbf{A}^{(i)}\cdot\nabla T^{p(i)} + \mathbf{q}^{*p(i)} \end{cases}$$
$$\begin{aligned} &T^p(\mathbf{x},t) = T^{0p} = T_p^0 - \nabla T^0\cdot\mathbf{v}^p \quad \mathbf{x}\in\Gamma_T; \\ &q_{nc}^p(\mathbf{x},t) = h\left(T^p - T_\infty^p\right) + \mathbf{q}_\Gamma\cdot\nabla_\Gamma v_n^p \quad \mathbf{x}\in\Gamma_c; \\ &q_n^{rp} = 4\sigma T^3\left(T^p + \nabla T\cdot\mathbf{v}^p\right) - \nabla q_n^r\cdot\mathbf{v}^p + \mathbf{q}^r\cdot\nabla_\Gamma v_n^p \quad \mathbf{x}\in\Gamma_r; \\ &q_n^{p(i)}(\mathbf{x},t) = q_n^{p(i+1)}(\mathbf{x},t) \quad \mathbf{x}\in\Gamma_N \\ &T_0^p(\mathbf{x},0) = T_{0p} - \nabla T_0\cdot\mathbf{v}^p \quad \mathbf{x}\in(\Omega\cup\Gamma). \end{aligned} \qquad (4)$$

Equations 2 and 4.

$$F_P = \int_0^{t_f} \left\{ \int_{\Gamma_T} \left[\gamma_{,T} \left(T_p^0 - \nabla_\Gamma T^0 \cdot \mathbf{v}_\Gamma^p - T_{,n}^0 v_n^p \right) + \gamma_{,q_n} \left(q_n^p - \mathbf{q}_\Gamma \cdot \nabla_\Gamma v_n^p \right) \right] d\Gamma_T + \right.$$

$$\int_{\Gamma_q} \left[\gamma_{,T} T^p + \gamma_{,q_n} \left(q_{np}^0 - \nabla_\Gamma q_n^0 \cdot \mathbf{v}_\Gamma^p - q_{n,n}^0 \cdot v_n^p \right) \right] d\Gamma_q + \int_{\Gamma_c} \left[\gamma_{,q_n} h \left(T^p - T_\infty^p \right) \right] d\Gamma_c + \int_{\Gamma_r \cup \Gamma_C} \gamma_{,T} T^p d(\Gamma_r \cup \Gamma_C) + \tag{5}$$

$$\left. \int_\Gamma (\Psi + \gamma_{,n} - 2H\gamma) v_n^p \, d\Gamma + \int_\Gamma \gamma_{,T_\infty} T_\infty^p \, d\Gamma + \int_\Sigma \right] \gamma \mathbf{v}^p \cdot \mathbf{v} \left. \right\} dt ; \qquad p = 1, 2, \ldots P.$$

$$\begin{cases} -\operatorname{div} \mathbf{q}^{a(i)} + f^{a(i)} = c^{(i)} \dfrac{dT^{a(i)}}{d\tau} & \mathbf{x} \in \Omega; \\ \mathbf{q}^{a(i)} = \mathbf{A}^{(i)} \cdot \nabla T^{a(i)} + \mathbf{q}^{*a(i)} \end{cases} \tag{6}$$

$$T^a(\mathbf{x}, \tau) = T^{0a}(\mathbf{x}, \tau) \quad \mathbf{x} \in \Gamma_T \; ; \; q_n^a(\mathbf{x}, \tau) = \mathbf{n} \cdot \mathbf{q}^a = h \left[T^a(\mathbf{x}, \tau) - T_\infty^a(\mathbf{x}, \tau) \right] \mathbf{x} \in \Gamma_c \; ;$$

$$\mathbf{n} \cdot \mathbf{q}^{ar} = q_n^{ar}(\mathbf{x}, \tau) \quad \mathbf{x} \in \Gamma_r ; \qquad T^a(\mathbf{x}, \tau = 0) = T_0^a(\mathbf{x}, \tau = 0) \quad \mathbf{x} \in (\Omega \cup \Gamma).$$

$$f^a(\mathbf{x}, \tau) = 0 \quad \mathbf{x} \in \Omega; \qquad T^a(\mathbf{x}, \tau = 0) = 0 \quad \mathbf{x} \in (\Omega \cup \Gamma); \qquad q^{*a}(\mathbf{x}, \tau) = 0 \quad \mathbf{x} \in \Omega;$$

$$T^{0a}(\mathbf{x}, \tau) = \gamma_{,q_n}(\mathbf{x}, t) \qquad \mathbf{x} \in \Gamma_T ; \qquad T_\infty^a(\mathbf{x}, \tau) = \frac{1}{h} \gamma_{,T}(\mathbf{x}, t) + \gamma_{,q_n}(\mathbf{x}, t) \qquad \mathbf{x} \in \Gamma_c ; \tag{7}$$

$$q_n^{ar}(\mathbf{x}, \tau) = \sigma \left[T^a(\mathbf{x}, \tau) \right]^4 ; \; T^a(\mathbf{x}, \tau) = \left[\frac{-\gamma_{,T}(\mathbf{x}, t)}{\sigma} \right]^{0,25} \qquad \mathbf{x} \in \Gamma_r .$$

$$F_p = \int_0^{t_f} \left\{ \int_{\Gamma_T} \left[\left(\gamma_{,T} + q_n^a \right) \left(T_p^0 - \nabla_\Gamma T^0 \cdot \mathbf{v}_\Gamma^p - T_{,n}^0 v_n^p \right) - \gamma_{,q_n} \mathbf{q}_\Gamma \cdot \nabla_\Gamma v_n^p \right] d\Gamma_T \right.$$

$$+ \int_{\Gamma_c} \left[T^a h T_\infty^p - T^a \mathbf{q}_\Gamma \cdot \nabla_\Gamma v_n^p - \gamma_{,q_n} h T_\infty^p \right] d\Gamma_c - \int_{\Gamma_r} T^a q_n^{rp} \, d\Gamma_r + \int_\Gamma (\Psi + \gamma_{,n} - 2H\gamma) v_n^p \, d\Gamma \tag{8}$$

$$\left. + \int_\Gamma \gamma_{,T_\infty} T_\infty^p \, d\Gamma + \int_\Sigma \right] \gamma \mathbf{v}^p \cdot \mathbf{v} \left. \right\} dt .$$

Equation 5, 6, 7 and 8.

Expressions that define the adjoint fields can be written according to the same source (see ***Equation 7***).

The time transformation is now necessary and the final time $t = t_f$ at the primary and additional problem is equivalent to the starting time at the adjoint problem $\tau = 0$. The first-order sensitivity expression has the form [8, 10] presents in ***Equation 8***.

The optimization problem is sensitivity oriented, i.e. first-order sensitivity expressions are introduced into the optimization conditions. The optimal design problem is defined as the minimization of the objective functional with the imposed inequality constraint of the structural cost C. Assuming the homogeneous structure in real problems, the structural cost is proportional to the area of domain Ω. Introducing the Lagrange functional in the form $F' = F + \chi \left(C - C_0 + \xi^2 \right)$ cf. [7] and the stationarity correlations, the following optimality conditions can be implemented:

$$\begin{cases} F_p = -\chi \int_\Omega u \, v_n^p \, d\Gamma. \\ \int_\Omega u \, d\Omega - C_0 + \xi^2 = 0. \end{cases} \tag{9}$$

Let us introduce two typical optimization functionals. The most applied is the measure of the heat flux density on the external boundary in the form:

$$G = \int_0^{t_f} \left[\int_\Gamma q_n d\Gamma \right] dt \; ; \; \Gamma \in \Gamma_{external} \tag{10}$$

Minimization of the above functional corresponds to designing a structure of optimal thermal insulation, whereas maximization is a condition of the optimal heat radiator.

The functional can also be a global measure of the maximum local temperature within the domain. The optimal shape is obtained by minimising the distribution of the state variable within the structure as show in ***Equation 11***.

Assuming $n \to \infty$, minimization of this functional provides equalization of the temperature distribution on the optimized boundary as well as minimizes its local maximum values. The troublesome first-

order sensitivity can be now implemented with respect to ***Equation 11***.

$$\frac{DG}{Db_p} = G_p = \frac{1}{n}(G_w)^{\frac{1-n}{n}} \frac{D(G_w)}{Db_p} \quad (12)$$

Numerical examples

Let us optimize the thickness of a external calender mantle made of a single material layer. The device is supplied with oil at a specific temperature which allows to maintain a constant temperature of the operating surface. Textiles are subjected to the finishing procedure by calendering at a working temperature of more than 220 ºC. The device should secure optimal heat transfer conditions on the external boundary. The basic quality criterion is to provide anequalized temperature distribution on the heating surface. Therefore let us minimize the objective functional described by ***Equation 11*** as a steady problem i.e. during an normal operation (see ***Equation 13***).

The mantle is made of a single layer of ferritic stainless, low-carbon alloy steel X6Cr17 acc. to ISO and EN 10088-3/1.4016 acc. to EN 10088-3. This steel is used to manufacture parts of machines working in the nitric acid industry, as well as the following branches: dairy, beverage, sugar, fruit and vegetable processing and the components of canteens and households. Steel is resistant to atmospheric corrosion and the corrosive action of all chemicals used during the finishing procedure of textiles i.e. natural water, water vapor, diluted cold organic acids, saline solutions, diluted alkaline solutions etc. The material is thermally isotropic of one-dimensional matrix of thermal conduction coefficients $\mathbf{A} = |\lambda| = 25\ \mathrm{Wm^{-1}K^{-1}}$ and volumetric heat capacity $c = 460\ \mathrm{Jkg^{-1}K^{-1}}$. The length of the mantle is an extension of the center line of the channel filled by heating oil, i.e. helix described by ***Equation 1***. The temperature of the oil varies along the central line from 280 °C at the input to 275 °C at the output. It follows that the boundary portion Γ_T is subjected to temperature $T(\mathbf{x}) = T^0(\mathbf{x})$, which varies linearly along the length, cf. ***Figure 2***. The external part of the mantle is subjected to thermal convection as well as thermal radiation to the surrounding temperature $T_\infty = 0$ °C and surface film conductance $h = 5\ \mathrm{Wm^{-2}K^{-1}}$. Let us introduce for simplicity the negligible initial heat flux density $\mathbf{q}^* = 0$. The primary problem is defined with respect to ***Equations 2*** as presented in ***Equation 14***.

$$G = \int_0^{t_f} \left\{ \left[\int_\Gamma \left(\frac{T}{T_{0L}} \right)^n d\Gamma \right]^{\frac{1}{n}} \right\} dt \ ; \ n \to \infty \qquad \Gamma \in \Gamma_{external}. \quad (11)$$

$$\min \left(G = (G_w)^{\frac{1}{n}} = \left[\int_\Gamma \left(\frac{T}{T_{0L}} \right)^n d\Gamma \right]^{\frac{1}{n}} ; \ n = 25 \right) \quad \Gamma \in \Gamma_C \cup \Gamma_r. \quad (13)$$

Equations 11, and 13.

The design variable is the thickness of the only material layer g, optimised by means of the direct approach, which is convenient for a small number of design variables. The additional structure is defined by ***Equations 4***, whereas the sensitivity expression is given by ***Equation 5***. The mean curvature of the external boundary Γ is zero because the cross-section of the external surface is a straight line. Introducing the conditions shown in ***Figure 2*** and the material derivatives of temperature $T^0_P = T_{0P}$, known in advance, we simplify these equations to those presented in the set of ***Equations 15***.

It is necessary to introduce additional constraints during the optimization procedure on the initial material thickness $g_{init} = 5 \cdot 10^{-2}$ m. The thickness is arbitrarily determined between a minimum equal to 20% of the initial to a maximum of 150% of the initial dimension. The optimization procedure is iterative. The cross-section of the calender mantle is approximated by means of the finite element net. The problem is two-dimensional and the elements are planar. The analysis step allows to introduce a regular net of rectangular finite elements based on 630 nodes. The synthesis step is performed by means of the external penalty function. The optimal thickness $g_{opt} = 4.53 \cdot 10^{-2}$ m is determined after 11 iteration steps, and the optimal functional is equal to 87.3% of the initial value.

Let us next optimize the external calender mantle as a multi-layer structure made of three different material layers. The heat-

$$-\mathbf{A}^{(i)} \cdot \mathrm{div}\left(\nabla T^{(i)}\right) = c^{(i)} \frac{dT^{(i)}}{dt} \quad \mathbf{x} \in \Omega; \qquad \begin{array}{l} T(\mathbf{x}) = T^0(\mathbf{x}) \quad \mathbf{x} \in \Gamma_T; \quad q^r_n(\mathbf{x}) = \sigma\, T(\mathbf{x})^4 \quad \mathbf{x} \in \Gamma_r; \\ q_{nc}(\mathbf{x}) = h\left[T(\mathbf{x}) - T_\infty(\mathbf{x})\right] \quad \mathbf{x} \in \Gamma_C. \end{array} \quad (14)$$

$$\begin{array}{l} -\mathbf{A}^{(i)} \cdot \mathrm{div}\left(\nabla T^{p(i)}\right) = c^{(i)} \dfrac{dT^{p(i)}}{dt} \quad \mathbf{x} \in \Omega; \\ T^p(\mathbf{x}, t) = -\nabla T^0 \cdot \mathbf{v}^p \quad \mathbf{x} \in \Gamma_T; \\ q^p_{nc}(\mathbf{x}, t) = h\left(T^p - T^p_\infty\right) + \mathbf{q}_\Gamma \cdot \nabla_\Gamma v^p_n \quad \mathbf{x} \in \Gamma_c; \\ q^{rp}_n = 4\sigma T^3\left(T^p + \nabla T \cdot \mathbf{v}^p\right) - \nabla q^r_n \cdot \mathbf{v}^p + \mathbf{q}^r \cdot \nabla_\Gamma v^p_n \quad \mathbf{x} \in \Gamma_r; \end{array} \quad (15)$$

$$\frac{D(G_w)}{Db_p} = (G_w)_p = \int_{\Gamma_C \cup \Gamma_r} \left[\frac{n}{T_{0L}} \left(\frac{T}{T_{0L}} \right)^{n-1} T^p + \left(\frac{T}{T_{0L}} \right)^n {}_n v^p_n \right] d(\Gamma_C \cup \Gamma_r) + \int_\Sigma \left(\frac{T}{T_{0L}} \right)^n \mathbf{v}^p \cdot \mathbf{v} \left[\right.$$

Equations 14, and 15.

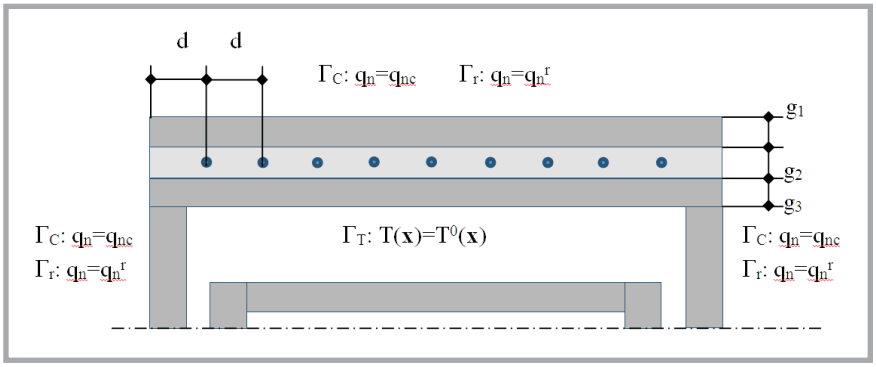

Figure 3. *Boundary conditions of three-layer calender mantle.*

$$\min\left(G=\int_0^{t_f}(G_w)^{\frac{1}{n}}\,dt=\int_0^{t_f}\left[\int_\Gamma\left(\frac{T}{T_{0L}}\right)^n d\Gamma\right]^{\frac{1}{n}}dt;\quad n=25\right)\quad \Gamma\in\Gamma_C\cup\Gamma_r \qquad (16)$$

$$f^a(x,\tau)=0\quad x\in\Omega;\qquad T^a(x,\tau=0)=0\quad x\in(\Omega\cup\Gamma);\qquad q^{*a}(x,\tau)=0\quad x\in\Omega;$$

$$T^{0a}(x,\tau)=0\qquad x\in\Gamma_T;\qquad T^a_\infty(x,\tau)=\frac{1}{h}\frac{n}{T_{0L}}\left(\frac{T}{T_{0L}}\right)^{n-1}\qquad x\in\Gamma_c;$$

$$q^{ar}_n(x,\tau)=\sigma\left[T^a(x,\tau)\right]^4;\ T^a(x,\tau)=\left[\frac{1}{\sigma}\frac{n}{T_{0L}}\left(\frac{T}{T_{0L}}\right)^{n-1}\right]^{0,25}\qquad x\in\Gamma_r; \qquad (17)$$

$$\frac{D(G_w)}{Db_p}=\int_0^{t_f}\left\{\int_{\Gamma_c}\left[T^a h T^p_\infty-T^a\mathbf{q}_\Gamma\cdot\nabla_\Gamma v^p_n\right]d\Gamma_c-\int_{\Gamma_r}T^a q^{np}_n\,d\Gamma_r+\int_{\Gamma_{ext}}\left(\frac{T}{T_{0L}}\right)^n{}_{,n}v^p_n\,d\Gamma_{ext}+\right.$$

$$\left.\int_\Sigma\left(\frac{T}{T_{0L}}\right)^n\mathbf{v}^p\cdot\boldsymbol{\upsilon}\right\}dt.$$

$$\max\left(G=\int_0^{t_f}\left[\int_\Gamma q_n d\Gamma\right]dt\right)\Rightarrow\min\left(G=-\int_0^{t_f}\left[\int_\Gamma q_n d\Gamma\right]dt\right);\ \Gamma\in\Gamma_C\cup\Gamma_r \qquad (18)$$

Equations 16, 17 and 18.

Table 1. *Initial and optimal dimensions of three-layer calender mantle designed for temperature equalization.*

Shape	Layer thickness, ×10^{-2} m			Distribution of heat sources d, ×10^{-2} m
	g_1 (alloy steel)	g_2 (sintered alloy)	g_3 (brass)	
Initial	2.5	3.5	1.0	10.0
Optimal	2.3	4.2	0.8	9.7

Table 2. *Initial and optimal dimensions of three-layer calender mantle designed as heat radiator.*

Shape	Layer thickness, ×10^{-2} m			Distribution of heat sources d, ×10^{-2} m
	g_1 (alloy steel)	g_2 (sintered alloy)	g_3 (brass)	
Initial	2.5	3.5	1.0	10.0
Optimal	1.9	2.9	0.7	10.2

ing medium (oil) has a variable inlet temperature according to the time function $T_i = 250 + \beta\ \mathrm{sqrt}(3\ t)$ and outlet temperature according to the time function $T_o = 220 + \beta\ \mathrm{sqrt}(2.8\ t)$, varying linearly along the helix. The optimality criterion is the equalized temperature on the operating surface determined by ***Equation 11***, see ***Equation 16***.

The internal layer is made of low-carbon alloy steel X6Cr17 as the high strength support element. The middle layer is made of sintered alloy of increased volumetric heat capacity,which is designed as a thermal stabilizer. The external brass shell contacts the textile and can provide the equalized temperature. The middle layer contains additional heating elements in the form of electrically heated conductors. For simplicity let us assume that they are perpendicular to the channel i.e. within cross-section there are heat point sources of transient capacity $f = 10e^{-t}$ Wm^{-1}. The internal layer has the same material parameters as previously. The sintered alloy is thermally isotropic of thermal conduction coefficient matrix $\mathbf{A} = |\lambda| = 110$ Wm^{-1}K^{-1} and volumetric heat capacity $c = 960$ Jkg^{-1}K^{-1}. The isotropic brazen layer hasthermal parameters $\mathbf{A} = |\lambda| = 110$ Wm^{-1}K^{-1} and $c = 395$ Jkg^{-1}K^{-1}. The surrounding temperature is $T_\infty = 0$ °C and the surface film conductance $h = 5$ Wm^{-2}K^{-1}. Again the primary problem has the form of ***Equation 2***.

The design variables are the thicknesses of material layers g_1, g_2 & g_3 and the distribution of heating elements is defined by the dimension d, cf. ***Figure 3***. The adjoint approach is introduced, which is suitable for a small number of objective functionals. The adjoint structure is described by ***Equation 6*** and ***7***, and the sensitivity expression by ***Equation 8***. Including $\gamma = \gamma(T)$, $f^p = \partial f/\partial b_p$, the set of conditions as well as assuming material derivatives of temperature $T^0{}_P = T_{0P}$ known in advance, ***Equation 7*** and ***8*** are simplified to the set of ***Equations 17*** form.

The transient optimization problem is solved for equidistant 20 steps of time from $t_{init} = 0$ to $t_{final} = 600$ s. It is necessary to introduce additional constraints to maintain the same sequence of layers and size distribution. The material thicknesses can change at each iteration no more than 10% of the initial value, whereas the distribution of heating elements is 30%.

$$f^{a}(\mathbf{x},\tau)=0 \quad \mathbf{x}\in\Omega; \qquad T^{a}(\mathbf{x},\tau=0)=0 \quad \mathbf{x}\in(\Omega\cup\Gamma); \qquad \mathbf{q}^{*a}(\mathbf{x},\tau)=0 \quad \mathbf{x}\in\Omega;$$

$$T^{0a}(\mathbf{x},\tau)=0 \qquad \mathbf{x}\in\Gamma_T; \qquad T^{a}_{\infty}(\mathbf{x},\tau)=1 \qquad \mathbf{x}\in\Gamma_c;$$

$$q^{ar}_{n}(\mathbf{x},\tau)=\sigma\left[T^{a}(\mathbf{x},\tau)\right]^{4}; \; T^{a}(\mathbf{x},\tau)=0 \qquad \mathbf{x}\in\Gamma_r; \tag{19}$$

$$G_p=\int_0^{t_f}\left\{\int_{\Gamma_c}\left[T^{a}hT^{p}_{\infty}-T^{a}\mathbf{q}_{\Gamma}\cdot\nabla_{\Gamma}v^{p}_{n}-hT^{p}_{\infty}\right]d\Gamma_c-\int_{\Gamma_r}T^{a}q^{rp}_{n}\,d\Gamma_r+\int_{\Gamma}q_{n,n}\,v^{p}_{n}\,d\Gamma+\int_{\Sigma}\left[q_n\,\mathbf{v}^{p}\cdot\boldsymbol{\upsilon}\right]\right\}dt\,.$$

Equation 19.

The optimization procedure is iterative. The analysis stage was determined using a rectangular finite element net of 900 nodes. At the synthesis step the external penalty function was introduced, the initial and optimal dimensions of which are shown in ***Table 1***. The optimal shape is determined after 17 iterations, and the optimal functional is equal to 92.8% of the initial value.

The results indicate that the sum of optimal thicknesses within the structure is greater than the initial. However, the optimum thicknesses of layers made of alloy steel and brass are thinner than the initial. Equalization of the temperature on the outer surface is secured by an increase in the thickness of the intermediate layer made of sintered alloy of 20% i.e. material which stabilizes the temperature. The distribution of heat sources is practically unchangeable, that is, the objective functional is not sensitive to a change in the dimension d.

The material layers within the three-layer calender mantle was alternatively optimized using the other objective functional. We introduce the same material parameters, thermal load and design variables. The optimality criterion is now maximization of the heat flux density on the external boundary portion. The optimization problem is defined according to ***Equation 9*** and shown in ***Equation 18***.

Again the primary problem has the form of ***Equation 2*** and the adjoint one ***Equation 6***. Expressions that define the adjoint fields can be determined according to ***Equation 7***, whereas the first-order sensitivity expression is obtained by ***Equation 8***. Both can be finally described in the form presented by the set of ***Equations 19***.

The optimization procedure is the same as described previously. The initial and optimal dimensions are shown in ***Table 2***. The optimal thicknesses and distribution d is determined after 12 iterations, and the optimal functional is equal to 85.1% of the initial value.

The principle of the heat radiator is that the thickness of the material layers should be as small as possible. Thus the optimal sum of material thicknesses is less than the same sum for the initial layers. Irrespective of the global dimension, each layer has a smaller optimal thickness than the initial one. Furthermore dimension "d" increased slightly with respect to the initial, but consistently has a negligible impact on the optimal solution.

Conclusions

Optimal heat transfer is a fundamental condition during the calendering process of different textile materials. This is achieved by shape optimization of the calender mantle, i.e. the thickness of material layers and the distribution of heating elements. Transient problems are complicated and should be solved approximately by means of different numerical methods. Steady problems can be considerably simplified, which is typical for some particular cases. Boundary conditions are formulated by application of real physical phenomena in the shaft during the calendaring process of textiles.

It can be concluded that optimal values of objective functionals are less than the initial. In addition, the optimal dimensions obtained are logical from an engineering point of view. The results presented show that the method discussed can be a promising tool to optimize the thermal conditions within the multi-layer calender shaft. Different constraints were used to improve the design results (for example, restrictions on the material thicknesses in each iteration, the maximal changes in the position of heating elements). The optimal shapes obtained during optimization are representative because the 3D spatial problem can be reduced to the calender cross-section by the plane of the symmetry, i.e. the planar 2D problem. The advantage is the little calculation time, the significant economic profit in relation to the other methods, and in fact an unlimited range of modeling the phenomena during calendering.

The calender mantle is optimized using the variational approach. Therefore the solution of the optimization procedure is simultaneously that of the specific physical problem. The base is always the carefully selected optimization criterion, that is, the choice of this problem. Calculations were performed using the two most frequent criteria on the operating surface: (1) the heat radiator problem (i.e. maximization of heat flux density), and (2) equalization of the temperature distribution and minimization of its local maximum values (i.e. minimization of the global measure of the maximum local temperature). Consequently the optimal thicknesses of the material layers determined cause an increase in the characteristics and functionality of the calender.

It is evident that the optimization results obtained should be verified practically. The problem is beyond the scope of the publication presented and will be introduced into the consecutive paper. The main difficulty is always the balance between the computational effort required to solve the problem and the complexity of the modelling. The basic 2D models as well as the finite element net applied are relatively uncomplicated and the effective calculation time is consequently insignificant. The more complicated shapes and spatial problems need the advanced 3D finite element net, due to which the calculation time grows significantly. Moreover the results can be verified for the existing calender shaft and the temperature measured within the structural points selected.

References

1. Sztajnowski S, Krucińska I, Sulak K, Wrzosek H, Bilska J. Effects of the artificial weathering of biodegradable spun-bonded PLA nonwovens in respect of their use in agriculture. *Fibres & Textiles in Eastern Europe* 2012; 20, 6B(96): 89-95.
2. Puchalski M, Krucińska I, Sulak K, Chrzanowski M, Wrzosek H. Influence of the calender temperature on the crystallization behaviors of polylactide spunbonded non-woven fabrics. *Textile Research Journal* 2013; 83, 17: 1775-1785.
3. Kuo Ch-FJ, Fang Ch-Ch. An Entire Strategy for Control of a Calender Roller System. Part I: Dynamic System Modeling and Controller Design. *Textile Research Journal* 2007; 77: 343-352.
4. Kuo Ch-FJ, Tu H-M. Gray Relational Analysis Approach for the Optimization of Process Setting in Textile Calendering. *Textile Research Journal* 2009; 79, 11: 981-992.
5. Midha VK. Study of stiffness and abrasion resistance of needle-punched nonwoven blankets. Journal of the Textile Institute 2011; 102, 2: 126-130.
6. Turant J. The optimal design of heat sources distribution in calender (in Polish). *Zeszyty Naukowe WSInf*. 2010; 9, 2: 65-71.
7. Dems K, Korycki R, Rousselet B. Application of the first- and second-order sensitivities in domain optimization for steady conduction problem. *Journal Therm. Stresses* 1997; 20: 697-727.
8. Korycki R. Two-dimensional shape identification for the unsteady conduction problem. *Structural and Multidisciplinary Optimization* 2001; 21, 4: 229-238.
9. Dems K, Korycki R. Sensitivity analysis and optimal design for steady conduction problem with radiative heat transfer. *Journal of Thermal Stresses* 2005; 28: 213-232.
10. Korycki R. Sensitivity analysis and shape optimization for transient heat conduction with radiation. *International Journal of Heat and Mass Transfer* 2006; 49 (13-14): 2033-2043.
11. Korycki R, Więzowska A. Modelling of the temperature field within knitted fur fabrics. *Fibres & Textiles in Eastern Europe* 2011; 84, 1: 55 – 59.
12. Li Y. The science of clothing comfort. *Textile Progress* 2001; 31, 1-2: 1-135. DOI: 10.1080/00405160108688951.

Received 05.11.2014 Reviewed 26.01.2015